Effects of I_{Kr} and I_{Ks} Heterogeneity on Action Potential Duration and Its Rate Dependence

A Simulation Study

Prakash C. Viswanathan, BE; Robin M. Shaw, PhD; Yoram Rudy, PhD

Background—A growing body of evidence suggests that heterogeneity of ion channel expression and electrophysiological characteristics is an important property of the ventricular myocardium. The 2 components of the delayed rectifier potassium current, I_{Kr} (rapid) and I_{Ks} (slow), play a dominant role in the repolarization of the action potential and are important determinants of its duration.

Methods and Results—In this report, the effects of heterogeneities of I_{Kr} and I_{Ks} on action potential duration (APD) and its rate dependence (adaptation) are studied with the use of the LRd model of a mammalian ventricular cell. Results demonstrate the importance of I_{Ks} density variations in heterogeneity of repolarization. Cells with reduced I_{Ks} (eg, mid-myocardial M cells) display long APD and steep dependence of APD on rate. Mechanistically, accumulation of I_{Ks} activation and increased sodium calcium exchange current, I_{NaCa}, secondary to Na^+ accumulation at a fast rate underlie the steep APD-rate relation of these cells. When cells are electrotonically coupled in a multicellular fiber through resistive gap junction, APD differences are reduced. The results demonstrate strong dependence of APD heterogeneity on the degree of intercellular coupling even in the normal physiological range. Highly reduced coupling maximizes APD heterogeneity.

Conclusions—Heterogeneity of I_{Ks}:I_{Kr} density strongly influences APD and its rate dependence. However, in the intact myocardium, the degree of gap-junction coupling may be an important factor that determines the manifestation of APD heterogeneity and dispersion of repolarization. The clinical significance of this study is in the context of repolarization abnormalities and associated arrhythmias (eg, long QT syndrome and torsade de pointes). **(*Circulation*. 1999;99:2466-2474.)**

Key Words: arrhythmia ■ action potentials ■ conduction ■ potassium ■ calcium channels

A growing body of evidence suggests that electrophysiological heterogeneity is an important property of ventricular myocardium. Variability of protein expression and/or electrophysiological function has been reported for the transient outward current,[1] the late sodium current,[2] and the slow[3] and rapid[4] components of the delayed rectifier current. Importantly, a subpopulation of cells (mid-myocardial M cells) has been described in the ventricular wall of the guinea pig,[5] canine,[6] and human.[7] The M cells display a longer action potential (AP) duration (APD) and a steeper dependence of APD on rate than the other (epicardial or endocardial) ventricular cell types. These cells also show greater responsiveness to interventions that prolong APD (eg, class III antiarrhythmic drugs)[8] and higher susceptibility to the development of arrhythmogenic early afterdepolarizations (EADs).

The 2 components of the delayed rectifier potassium current, I_{Kr} (rapid) and I_{Ks} (slow), play a dominant role in AP repolarization.[9,10] The physiological heterogeneity of repolarization and of APD across the ventricular wall has been associated with heterogeneity in the relative densities of I_{Kr} and I_{Ks}.[3] In particular, I_{Ks} density in M cells is lower than in other cell types. The relative densities of functional I_{Kr} and I_{Ks} channels can be altered by disease (eg, LQT1, LQT5, and LQT2, forms of the long QT syndrome[11,12]) or by class III agents that preferentially block one of these currents.

It is important, therefore, to answer the following question: What are the electrophysiological consequences, in terms of APD and its rate dependence, of heterogeneities in the relative densities of I_{Kr} and I_{Ks}? In this report, we use theoretical simulations to investigate this phenomenon and its ionic mechanism in isolated cells and in the multicellular tissue.

Received September 18, 1998; revision received December 7, 1998; accepted January 11, 1999.

From the Cardiac Bioelectricity Research and Training Center, Department of Physiology and Biophysics (P.C.V., Y.R.) and Department of Biomedical Engineering (R.M.S., Y.R.), Case Western Reserve University, Cleveland, Ohio.

Presented in part at the 69th Scientific Sessions of the American Heart Association, New Orleans, La, November 10–13, 1996, and published in abstract form (*Circulation*. 1996;94[suppl I]:I-712 and *Biophys J*. 1997;72:MP131–MP131).

Correspondence to Dr Yoram Rudy, Director, Cardiac Bioelectricity Research and Training Center, 505, Wickenden Bldg, Case Western Reserve University, Cleveland, OH 44106-7207. E-mail yxr@po.cwru.edu

Circulation **is available at http://www.circulationaha.org**

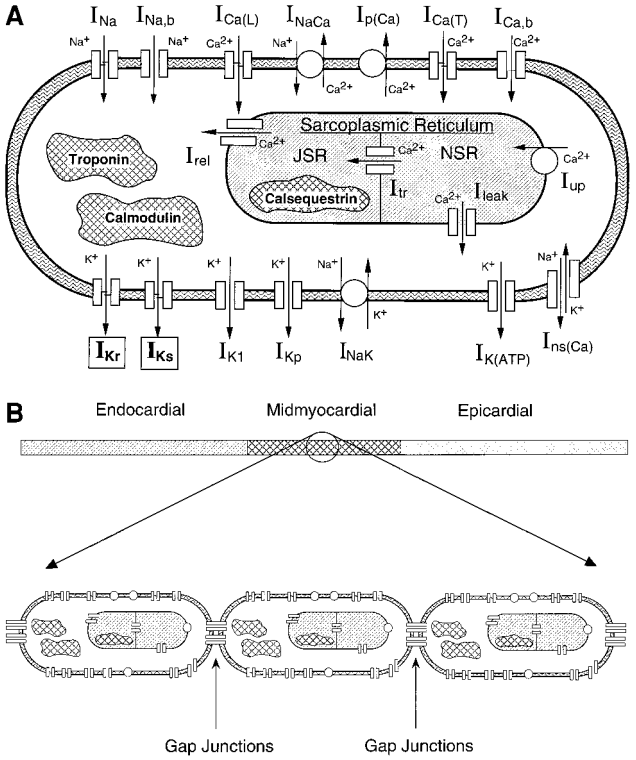

Figure 1. A, Schematic of LRd mammalian ventricular cell model. Detailed description is provided in References 10, 13, and 14. I_{Kr} and I_{Ks}, the currents that are modified to introduce cellular heterogeneity, are highlighted in the figure. B, Multicellular cardiac fiber composed of LRd cells interconnected by gap junctions. Spatial heterogeneities in density of I_{Ks} are introduced to simulate different cell types found in myocardium.

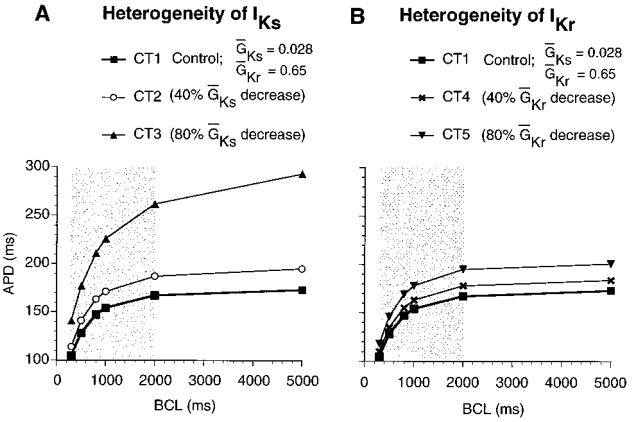

Figure 2. Effects of heterogeneities in I_{Ks} or I_{Kr} density on APD and its rate dependence. A, Effect of changes in density of I_{Ks} for constant I_{Kr} density. B, Effect of changes in density of I_{Kr} for constant I_{Ks} density. Shaded region indicates physiological heart rates.

Methods

Cell Model

The theoretical dynamic model of a mammalian ventricular AP (Figure 1A), the LRd model, provides the basis for the simulations in this study.[13,14] In this model, the AP is numerically constructed from ionic processes that are formulated on the basis of experimental data obtained mostly from the guinea pig. The model also accounts for processes that regulate ionic concentration changes. I_{Ks} was recently shown to display 2 (fast and slow) activation processes.[15] The slow time constant is larger than the fast time constant by a factor of 3 to 5. We incorporated this property into the formulation of I_{Ks} by introducing an activation X_{s2} gate, whose time constant is 4 times that of X_{s1} (which corresponds to X_s in Reference 10). The calcium dependence of I_{Ks} was modified on the basis of the recent study by Nitta et al.[16] Formulation of I_{Ks} is provided in the Appendix. Heterogeneities of I_{Kr} and I_{Ks} densities were introduced by altering their maximum conductances, $\bar{G}Kr$ and $\bar{G}Ks$. In view of recent findings regarding continuous Ca^{2+} release from the sarcoplasmic reticulum (SR), we have also modified the formulation of Ca^{2+} handling (Appendix). The modified formulation prevents nonphysiological discontinuities and oscillation(s) of $[Ca^{2+}]_i$ under extreme conditions. A detailed description of the cell model and its equations is provided in References 10, 13, and 14.

Simulation Protocols

Adaptation curves (the steady-state dependence of APD on rate) were obtained by pacing the cell at a constant cycle length (CL) for 5 minutes to achieve steady state, followed by a step increase to the next CL. APDs were obtained for CL of 300, 500, 800, 1000, 1500, 2000, and 5000 ms. APD was measured between the time of stimulus onset and 90% repolarization (APD_{90}). All computations were performed at a simulated temperature of 37°C.

Multicellular Fiber Model

The theoretical fiber[17] (Figure 1B) used in this study is composed of 190 ventricular cells, each of LRd formulation. The fiber contains an endocardial region (cells 1 to 80), M-cell region (cells 81 to 110), and an epicardial region (cells 111 to 190). Gap junction conductance (g_j) is homogeneous throughout the fiber and for different simulations varies from 2.5 μS (normal coupling[18]) to 0.025 μS (poor coupling). The fiber is stimulated or paced from cell 1.

Results

Relative Density of I_{Ks} and I_{Kr} Has a Major Effect on APD and Its Rate Dependence

We have previously shown[10] that modulation of I_{Kr} or I_{Ks} results in dramatic changes in the APD. Figure 2 shows the effect of different I_{Ks}:I_{Kr} density ratios on APD and its rate dependence. In panel A, I_{Ks} density is varied, whereas I_{Kr} density is held constant. In panel B, I_{Ks} density is maintained, whereas I_{Kr} density is varied. Cell type 1 (CT1) serves as control. In panel A, I_{Ks} is decreased by 40% and 80% in CT2 and CT3 cells, respectively. In panel B, I_{Kr} is similarly decreased in CT4 and CT5 cells. At a basic cycle length (BCL) of 5000 ms, the increase of APD between CT3 and CT1 (I_{Ks} variations) is 70%, whereas between CT5 and CT1 (I_{Kr} variations) it is only 16%. This dominant effect of I_{Ks} is consistent with the experimental findings[3] that transmural heterogeneity of I_{Ks} density (it is greatly reduced in the M cells) plays a major role in the transmural heterogeneity of APD (I_{Kr} density was found to be relatively uniform across the ventricular wall).

Guided by these findings, the following simulations of APD heterogeneity will focus on the role of I_{Ks}. It should be mentioned, however, that the simulated variations of I_{Kr} in Figure 2B are likely to have greater effects on APD if they occurred on the background of a significantly smaller I_{Ks}. Such a situation can arise when I_{Kr} in M cells is suppressed by mutation (eg, LQT2) or by a specific blocking agent.

Figure 3 shows the effect of pacing frequency on APD for 3 different I_{Ks}:I_{Kr} density ratios (I_{Kr} was kept constant). Figure

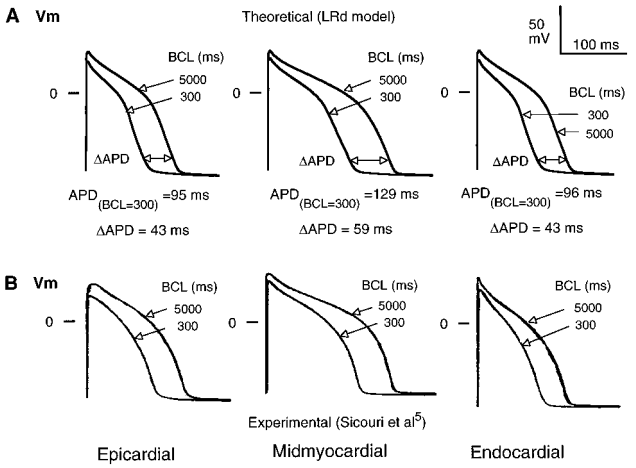

Figure 3. APs at fast and slow pacing rates for different densities of I_{Ks}. Computed (A) and experimentally recorded (B) APs at BCL of 300 and 5000 ms, respectively.

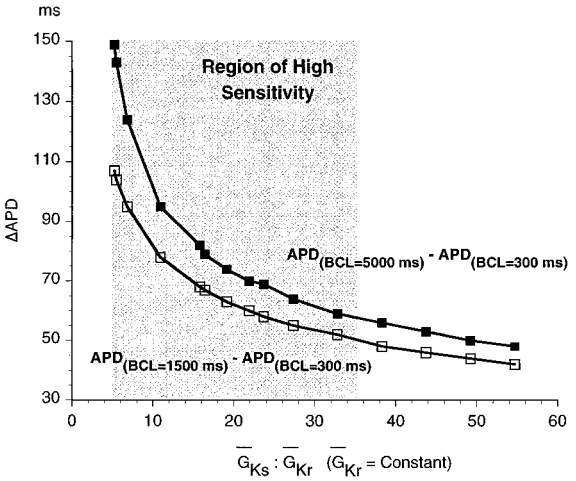

Figure 4. Effect of different I_{Ks}:I_{Kr} density ratios on APD adaptation to rate changes. A decrease in $\bar{G}Ks$:$\bar{G}Kr$ ratio (caused by decrease in I_{Ks} density) augments the adaptability (ΔAPD) of cells. Curve is steep for $\bar{G}Ks$:$\bar{G}Kr$ in the range 5 to 35 (shaded region). ΔAPD is shown for BCL change from 5000 to 300 ms (upper curve) and from 1500 to 300 ms (lower curve).

3A shows computed steady-state APs at fast and slow pacing frequencies (BCL of 300 and 5000 ms, respectively) in comparison to experimentally recorded APs (Figure 3B) from the 3 regions of the guinea pig ventricular wall.[5] The model accurately simulates the APD at the fast and slow rates for the different cell types on the basis of I_{Ks} heterogeneity. At a BCL of 300 ms, experimentally measured APDs[5] are 102±21, 136±9, and 95±15 ms in epicardial cells, M cells, and endocardial cells, respectively; the corresponding simulated APDs computed from the model are 95, 129, and 96 ms. At a BCL of 5000 ms, measured APDs are 133±14, 185±24, and 135±13 ms in epicardial cells, M cells, and endocardial cells; corresponding simulated APDs are 138, 188, and 139 ms. These values indicate a much longer APD and a slightly more accentuated dependence of APD on stimulation frequency in the M cells compared with either epicardial or endocardial cells.

The presence of transitional cells and heterogeneous APD even within the same cell type (see Figure 1B of Reference 3) indicates that there is no unique value of I_{Ks}:I_{Kr} density ratio that is associated with each cell type. Instead, there is wide range of density ratios in the myocardium that result in a distribution of APDs and their rate dependence. Figure 4 compiles the effects of different I_{Ks}:I_{Kr} density ratios on the adaptation of APD to rate changes (adaptation: $\Delta APD = APD_{(slow)} - APD_{(fast)}$). A decrease in $\bar{G}Ks$:$\bar{G}Kr$ (introduced by decreasing $\bar{G}Ks$) increases ΔAPD. The slope of the curve is steep for $\bar{G}Ks$:$\bar{G}Kr$ in the range from 5 to 35 (shaded region), indicating a strong effect of I_{Ks}:I_{Kr} heterogeneity on APD adaptation in this range. It is to be noted that these studies were conducted assuming uniform I_{Kr} density, consistent with the experimental findings.[3] We choose to focus on this range in the mechanistic investigation of APD adaptation because in this range the effect of changing I_{Ks} density is most significant. Interestingly, Figure 5 shows that for $\bar{G}Ks$:$\bar{G}Kr$ ratio in this range, the adaptation curves are in very good agreement with experimentally recorded adaptation curves from the human left ventricle.[7] Figure 5A also extends the simulated adaptation curves (dotted) to BCLs ranging from 300 to 1000 ms (a range of human basal heart rates). Experimental data from human myocytes for this range are currently unavailable.

Figure 6 shows simulated APs of the 3 cell types at a BCL of 2000 ms (A), together with the associated I_{Kr} (B) and I_{Ks} (C). We label the simulated cell types with density ratios $\bar{G}Ks$:$\bar{G}Kr$=23:1, 15:1, and 7:1 as epicardial cells, endocardial cells, and M cells, respectively. It is important to emphasize that this classification is based only on I_{Ks}:I_{Kr} density differences and the resulting heterogeneity of APD and its rate dependence (the focus of this report). Other differences between these cell types (eg, the presence of a large I_{to} in epicardial cells of certain species and the associated "spike and dome" morphology of their AP) are not considered here. It is observed from the figure that the APD of the M cell is longer than that of the epicardial cell. I_{Ks} is significantly smaller in the M cell (Figure 6C), starting from the early

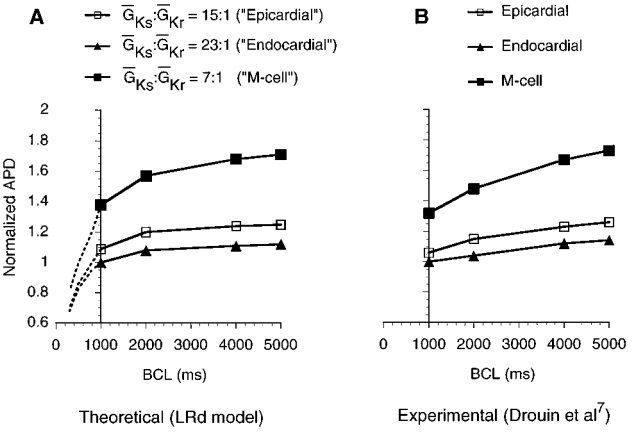

Figure 5. Normalized APD adaptation curves. A, Simulated adaptation curves obtained with the use of 3 $\bar{G}Ks$:$\bar{G}Kr$ ratios in the steep range of the curve of Figure 4. B, Experimentally recorded APD adaptation curves from epicardial, midmyocardial, and endocardial regions of human ventricle. Dotted lines in A extend adaptation curves to physiological heart rates (BCLs of 300 to 1000 ms) not available experimentally.

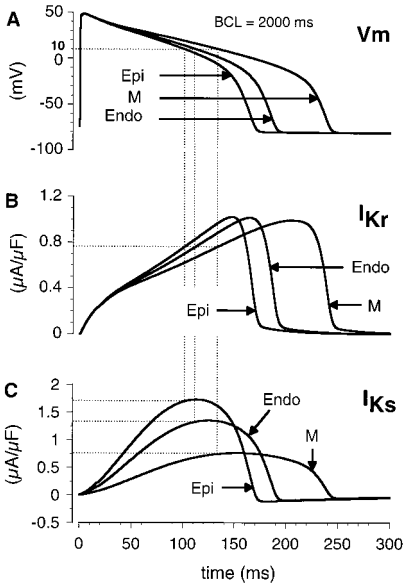

Figure 6. Heterogeneity of APD in 3 cell types in relation to I_{Kr} and I_{Ks}. Simulated APs of 3 cell types at BCL of 2000 ms (A) with corresponding I_{Kr} (B) and I_{Ks} (C). Dotted lines denote magnitudes of I_{Kr} and I_{Ks} at membrane potential of 10 mV. Epi indicates epicardial; M, M cell; and Endo, endocardial.

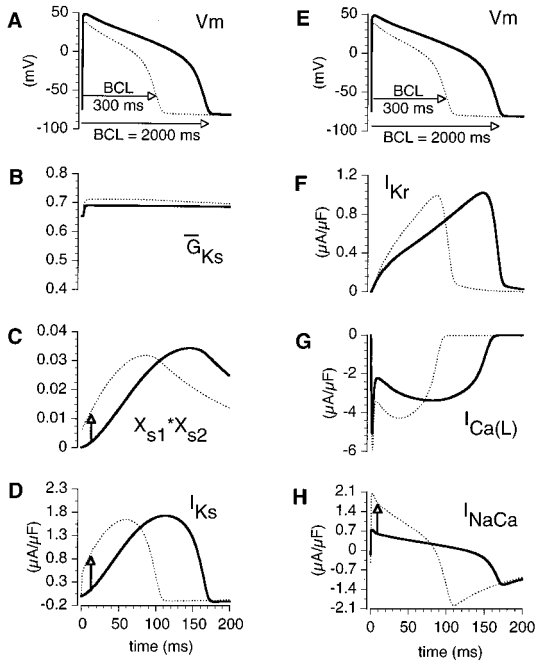

Figure 8. Mechanism of APD adaptation. A and E, Computed APs for slow pacing (bold line, BCL=2000 ms) and fast pacing (dotted line, BCL=300 ms) with corresponding $\bar{G}Ks$ (B), I_{Ks} activation $X_{s1} \cdot X_{s2}$, (C), I_{Ks} (D), I_{Kr} (F), $I_{Ca(L)}$ (G), and I_{NaCa} (H). Fast pacing increases I_{Ks} as the result of residual activation (arrows in D and C, respectively). Outward I_{NaCa} also increases (arrow in H) as the result of $[Na^+]_i$ accumulation.

phase of the AP, and attains a much smaller peak magnitude during the course of the AP. I_{Kr} (Figure 6B) appears to be smaller during the plateau phase of the AP in the M cell. However, it should be noted that the smaller I_{Kr} during this phase merely reflects the different time course of the AP.

Figure 7 shows simulated APs of the 3 cell types for a wide range of BCLs, superimposed to facilitate comparison. At a BCL of 300 ms, all 3 cell types display relatively short APs of similar APD (105, 113, and 135 ms for epicardial cells, endocardial cells, and M cells, respectively). With the slowing of pacing rate, the APD of the M cell is prolonged much more than that of the epicardial or endocardial cells, demonstrating a steeper dependence of APD on rate (greater adaptation). At a BCL of 2000 ms the APD of epicardial cells, endocardial cells, and M cells are 168, 188, and 240 ms, respectively. An important observation is that the effect of I_{Ks} heterogeneity (reduced I_{Ks} in M cells) is to prolong phase 3 repolarization without significantly affecting the plateau.

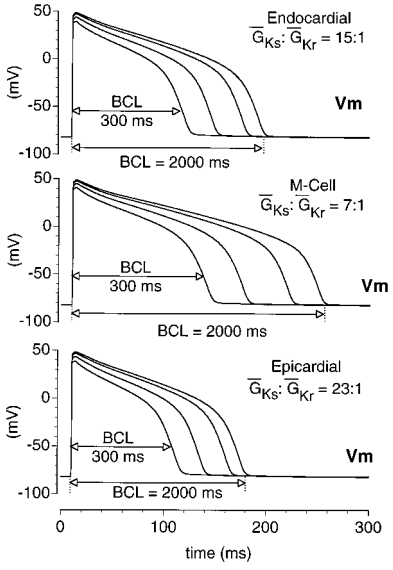

Figure 7. Rate dependence of APD in 3 cell types. M cells prolong their APD dramatically compared with epicardial and endocardial cells with slowing of stimulation rate. APs at progressively decreasing rate (BCL=300, 500, 1000, and 2000 ms) are shown for each cell type.

I_{Ks} and I_{NaCa} Play an Important Role in APD Adaptation and in Greater Adaptability of M Cells

The ability of cardiac myocytes to adjust their APD to changes in pacing frequency is termed adaptation. The most prominent effect of decreasing BCL is shortening of APD (Figures 2, 3, and 7). To investigate the mechanism of APD adaptation we examined selected transmembrane currents (I_{Kr}, I_{Ks}, $I_{Ca(L)}$, and I_{NaCa}) that play a role during the plateau and repolarization phases of the AP. Figure 8 shows simulated APs (panels A and E); corresponding ionic currents: I_{Ks} (D), I_{Kr} (F), $I_{Ca(L)}$ (G), and I_{NaCa} (H); maximal conductance of I_{Ks}, $\bar{G}Ks$ (B); and I_{Ks} activation, $X_{s1} \cdot X_{s2}$ (C). All parameters are shown for 2 different BCLs (300 ms and 2000 ms). The upstroke of the APs are aligned to facilitate comparison.

I_{Kr} is similar at the 2 frequencies (panel F, differences secondary to APD differences should not be considered and currents should be compared at the same V_m). Due to the slow kinetics of I_{Ks}, there is residual activation at the onset of the upstroke (arrow in Figure 8C). $\bar{G}Ks$, which depends on intracellular calcium, is not significantly altered (Figure 8B) at the fast rate. For $[Ca^{2+}]_i$=0.12 μmol/L (resting level), $\bar{G}Ks$

is 0.6495 ms/μF. At a steady-state BCL of 300 ms, peak $[Ca^{2+}]_i$ is 1.5 μmol/L. For this concentration, the value of $\bar{G}Ks$ is 0.6912 ms/μF, which is not significantly different from the resting value (an increase by only 6.5%). Therefore elevation of $[Ca^{2+}]_i$ at rapid rates has only a minor augmenting effect on I_{Ks}. The accumulation of I_{Ks} activation caused by incomplete deactivation is therefore the main cause of the larger I_{Ks}, which (together with increased outward I_{NaCa}; see below) acts to shorten the APD at a shorter BCL (arrow in Figure 8D). The greater cumulative activation of I_{Ks} at the time of stimulation for the short BCL is reflected in the instantaneous jump (Figure 8D) in the current at the onset of depolarization. The greater peak I_{Ks} at a longer BCL should not be considered in the comparison, as it is merely a consequence of the longer AP (because the membrane is depolarized for a longer duration, I_{Ks} is activated for a longer time and, in the absence of inactivation, reaches a greater peak current).

$I_{Ca(L)}$ (Figure 8G) has a larger plateau magnitude at the short BCL because of a larger driving force arising from a more negative plateau potential. Because $I_{Ca(L)}$ is an inward current, this would act to prolong the AP rather than shorten it. Therefore this current cannot contribute to APD shortening. However, at the short BCL, I_{NaCa} (Figure 8H), is predominantly outward ("reverse-mode") during the plateau phase. I_{NaCa} is regulated by $[Ca^{2+}]_i$ and $[Na^+]_i$. Elevation of $[Ca^{2+}]_i$ increases inward I_{NaCa}, whereas elevation of $[Na^+]_i$ increases outward I_{NaCa}. Fast pacing results in accumulation of $[Ca^{2+}]_i$ and $[Na^+]_i$. Our simulations show that the net effect of ion accumulation is a larger outward I_{NaCa} than control conditions (no accumulation). The increased outward I_{NaCa} (arrow in Figure 8H) acts to shorten the APD at the shorter BCL. Initially, the magnitude of this current appears to be greater than that of I_{Ks} (Figure 8D) at the fast rate. However, this current diminishes relatively quickly, reverses direction, and becomes a relatively large depolarizing current. This direction reversal limits the role of I_{NaCa} in APD shortening. However, this current still remains a participant in the APD adaptation process.

The results of Figure 8 provide insight into the processes that underlie adaptation. In Figure 9, we attempt to explain the greater adaptability of cells with lower I_{Ks} density (eg, M cells). Transmembrane currents computed from epicardial and M cells are compared at 2 different frequencies, fast (BCL=300 ms) and slow (BCL=2000 ms). Figure 9 shows plots of the APs (Figure 9A), the activation kinetics of I_{Ks} (Figure 9B), and I_{Ks} current (Figure 9C). It is seen from Figure 9B that at a shorter BCL, $X_{s1} \cdot X_{s2}$ is greater in the M cell than in the epicardial cell, reflecting a greater degree of activation and of channel availability. Activation is greater because of the longer APD and shorter time (diastolic interval) between complete repolarization and the next stimulus, which results in less deactivation and greater residual activation ($X_{s1} \cdot X_{s2}$) at the time of the next stimulus. This results in a greater relative increase of I_{Ks} at smaller BCL in the M cell (128%) than in the epicardial cell (33%). The greater increase of channel availability on BCL shortening in the M cell is not evident from the plot of I_{Ks} itself (Figure 9C), because I_{Ks} appears to be smaller in the M cell than in the epicardial cell. This simply reflects the smaller density of I_{Ks} in the M cell. The important observation is the greater percentage increase of I_{Ks} in the M cell (128% compared with 33% in the epicardial cell) on BCL shortening, which accounts for the greater adaptability. Due to a smaller total repolarizing current in the M cell (reflecting the smaller I_{Ks} density), any change in outward current magnitude, albeit small, will have a significant effect on the APD.

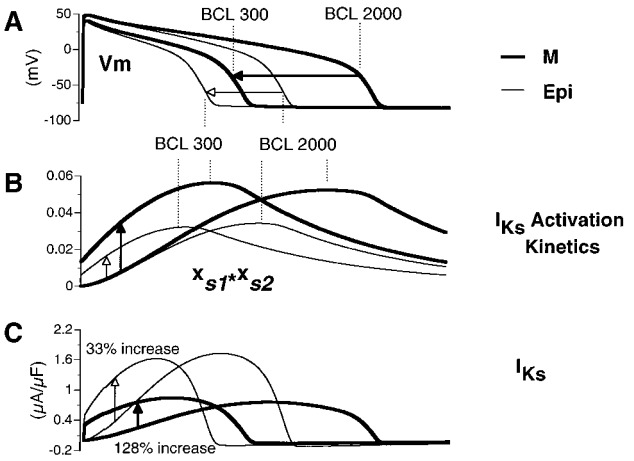

Figure 9. Mechanism of greater adaptability of M cells to changes in stimulation rate. A, Computed APs of epicardial (thin line; Epi) and M cell (bold line) at slow (BCL=2000 ms) and fast (BCL=300 ms) rates. B, $X_{s1} \cdot X_{s2}$ (I_{Ks} activation) displays greater residual value in M cell than in epicardial cell (compare black and white arrows). C, As a result of greater residual activation, there is a greater relative increase of I_{Ks} in M cell (128% compared with only 33% in epicardial cell).

I_{NaCa} (not shown in Figure 9) also plays a role in the greater adaptability of M cells. The Na^+-Ca^{2+} exchanger is transiently outward during the initial phase of the AP because of a transient increase in $[Na^+]$ influx through I_{Na}. However, at fast stimulation rates, accumulation of $[Na^+]_i$ increases the magnitude and duration of the transient outward component of I_{NaCa} (as seen in Figure 8H), thereby increasing the total repolarizing current. As stated previously, because of a smaller total repolarizing current in the M cell, any change in this current (in this case due to an increased outward I_{NaCa} resulting from an elevated $[Na^+]_i$) causes a significant change in APD.

Effect of Gap-Junction Coupling on APD

In the preceding sections we focused on understanding the mechanisms underlying the differences in APD and its rate dependence between isolated cells of the different types. However, in the intact heart, the cells are coupled through gap junctions and are subject to electrotonic interactions that affect their behavior. In this section we study the effects of intercellular coupling on APD and its rate dependence in the context of myocardial heterogeneity.

Figure 10A shows APDs along a multicellular fiber containing endocardial, M, and epicardial regions for different degrees of gap-junction coupling. The horizontal bold lines indicate APDs obtained from each cell type in isolation, in the absence of gap-junction coupling effects. For normal coupling of g_j=2.5 μS (velocity=56 cm/s, typical for propaga-

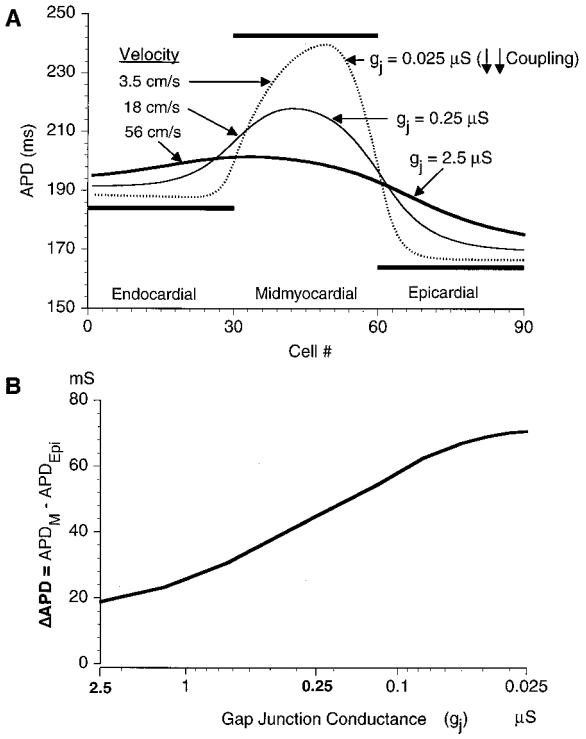

Figure 10. A, Effect of gap-junction coupling on APD heterogeneity. APDs along the multicellular fiber are shown (APD dispersion). Bold line corresponds to g_j=2.5 μS, thin line corresponds to g_j=0.25 μS, and dotted line corresponds to g_j=0.025 μS. Bold horizontal line in each region denotes single cell APD. B, Effect of different degrees of coupling on APD dispersion. ΔAPD shows steep dependence on gap junction conductance in normal physiological range (shaded region).

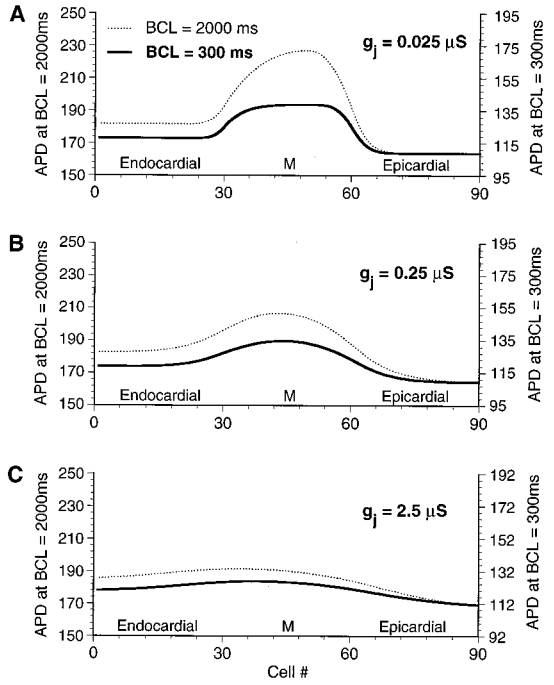

Figure 11. Rate dependence of APD dispersion along multicellular fiber. APD dispersion along fiber for very poor gap-junction coupling (A) and for 2 values of coupling in normal physiological range (B and C). Thick curves correspond to fast pacing (BCL=300 ms); dotted curves correspond to slow pacing (BCL=2000 ms).

tion along fibers), APD differences (dispersion) between the 3 cell types are greatly reduced compared with the isolated cell case. For this value of gap-junction coupling, the APD difference between M cells and epicardial cells is only 18 ms (differences are computed between middle cells of the respective regions). This is reflected in the figure by the relatively flat APD curve (bold line) along the fiber. However, with reduced coupling, APD differences increase sharply. At g_j=0.25 μS (velocity=18 cm/s, typical for propagation transverse to fibers), the APD difference between M cells and epicardial cells increases to 44 ms. When cells are very poorly coupled, APDs approach isolated cell values, resulting in a marked dispersion of APD along the fiber. At g_j=0.025 μS (velocity=3.5 cm/s, observed under pathological conditions such as infarction), APD difference between M cells and epicardial cells in the fiber increases to 71 ms (90 ms in the isolated cells).

The importance of intercellular coupling is better illustrated in Figure 10B, which compiles the effects of different gap-junction conductances on APD differences between M cells and epicardial cells in a fiber (ΔAPD between middle cells of each region). A 10-fold decrease in coupling (2.5 to 0.25 μS) increases dispersion of APD (ΔAPD) from 18 to 44 ms, demonstrating a steep dependence of ΔAPD on gap-junction coupling conductance in the physiological range. The simulations of Figure 10 were limited to an action potential elicited by a single stimulus, a protocol that tends to maximize APD differences. This protocol approximates certain pathological conditions such as extreme bradycardia or a postpause AP. Under such circumstances, APD differences would indeed be maximized. In the normal beating heart, the myocardium is subject to periodic stimulation. The following section addresses the issue of APD dispersion during periodic beating by characterizing the rate dependence of APD heterogeneity in the multicellular fiber.

Figure 11 shows the dispersion of APD along the fiber for 3 degrees of gap-junction coupling (top to bottom panels) during fast (BCL=300 ms, bold line) and slow (BCL=2000 ms, dotted line) pacing. It is observed that an increase in rate results in shortening of APD in all the 3 cell types. It is also observed that at the faster rate, APD differences along the fiber (dispersion) are reduced. The reduced dispersion is reflected in the flattening of the APD curve along the fiber at the fast rate compared with the slow rate. This behavior is similar to that of the isolated cells, in which at fast rates APDs of the 3 cell types converge (Figures 2 and 7). The mechanism of rate-dependent shortening of APD in the multicellular fiber is the same as in the isolated cells, that is, accumulation of I_{Ks} and a greater outward I_{NaCa} at fast rates.

Discussion

This study examines the effects of I_{Kr} and I_{Ks} heterogeneities on APD and its rate dependence and investigates the ionic mechanisms that underlie these phenomena. There is growing evidence that heterogeneities of these currents exist not only transmurally across the ventricular wall[6] but also in different regions of the ventricle.[4] The significance of this study lies in

this broad context of heterogeneities in channel density, although special emphasis is on transmural heterogeneity (the presence of M cells in the mid-myocardium), a case that has been extensively studied and very well characterized experimentally.

Our results demonstrate that changes in I_{Ks}:I_{Kr} density ratios result in heterogeneity of the repolarization properties of cells. A smaller density of I_{Ks} lengthens APD and results in greater prolongation of APD with slowing of stimulation rate, a behavior typical of the recently characterized M cells in the deep subepicardium. This study provides mechanistic insights into the rate-dependent shortening of APD (adaptation) and the greater adaptability of cells with reduced I_{Ks} density (eg, M cells) to changes in rate. Important findings include: (1) The relative density of I_{Kr} and I_{Ks} plays an important role in determining APD and its rate dependence. A smaller density of I_{Ks} can account for the distinct APD characteristics of M cells. (2) I_{Ks} and I_{NaCa} play an important role in APD adaptation to rate changes and in the greater adaptability of cells with reduced I_{Ks} density. (3) APD shortening at fast rates involves accumulation of I_{Ks} activation and augmentation of I_{NaCa}. Increase in I_{Ks} conductance secondary to intracellular Ca^{2+} accumulation has a negligible effect. (4) When cells are electrotonically coupled, the degree of intercellular (gap-junction) coupling plays a major role in determining APD heterogeneity and its rate dependence in the multicellular tissue. APD dispersion increases sharply with reduced coupling, approaching the isolated cells' APD differences when coupling is poor. (5) For normal coupling (typical to propagation along fibers), APD dispersion can reach a maximum value of 18 ms. With a 10-fold decrease in coupling (as observed transverse to fibers in the anisotropic myocardium), APD dispersion increases to a maximum value of 44 ms. These values decrease with increasing rate of stimulation.

Small I_{Ks} Density Can Account for Distinct APD Characteristics of M Cells: I_{Ks} and I_{NaCa} Underlie APD Adaptation and Greater Adaptability of M Cells

Rate-dependent shortening of APD is an important property of cardiac myocytes. Abrupt shortening of APD caused by a premature stimulus (APD restitution) has been shown to result from incomplete deactivation of I_{Kr} and I_{Ks}.[10] Steady-state shortening (APD adaptation) is also thought to be mainly due to incomplete deactivation and accumulation of ionic currents, in particular the slow delayed rectifier potassium current, I_{Ks}. Jurkiewicz et al[19] have measured an increased I_{Ks} at fast heart rates, lending support to this hypothesis.

From simulations conducted in this study we have determined that I_{Ks} accumulation at fast rates can explain the shortening of APD during adaptation. Because of the slow deactivation kinetics of I_{Ks}, there is residual activation at the onset of the succeeding AP that accumulates at fast rates, increasing the probability of the channel being in an open state. This is reflected in an instantaneous jump in I_{Ks}, as observed in Figure 8D (arrows). The resulting greater I_{Ks} acts to shorten the APD at fast rates.

An increase in heart rate results in a progressive rise in $[Na^+]_i$,[20] accompanied by an increase in the strength of contraction and shortening of the AP.[21] The I_{NaCa} has been implicated in the sodium-induced changes in contraction as well as the rate-dependent shortening of AP.[21] As seen in Figure 8H, outward I_{NaCa} increases at fast rates during the initial plateau phase of the AP and contributes to the observed rate-dependent shortening of the AP. Other plateau currents ($I_{Ca(L)}$ and I_{Kr}) do not play an important role in APD adaptation.

M cells have a steeper APD-rate relation than epicardial or endocardial cells. Investigation into this behavior has highlighted the importance of a reduced total repolarizing current in the M cells. As seen in the simulations, rapid pacing causes abbreviation of the APD as the result of increase in the repolarizing currents I_{Ks} and I_{NaCa}. This is true for all cell types, but the effect on APD is much greater in the M cells because it occurs on the background of a much smaller total repolarizing current.

Importance of Gap-Junction Coupling in Determining APD Heterogeneity in Multicellular Tissue

The unique repolarization properties of isolated M cells are widely accepted; however, controversy still exists over the extent to which heterogeneity in repolarization is expressed across the normal ventricular wall.[22,23] This is an important issue with major implications to the mechanism of arrhythmias associated with delayed and presumably nonuniform ventricular repolarization (eg, torsade de pointes). The simulations conducted in this theoretical study, in which gap-junction coupling and ion channels could be simultaneously controlled and systematically varied, provide valuable insights into APD heterogeneity. Our study highlights the important influence of gap-junction coupling on the manifestation of APD heterogeneity in the multicellular tissue. Small changes in intercellular coupling have a profound effect on APD dispersion (Figure 10B). This theoretical finding is consistent with a recent experimental observation made with optically recorded APs.[24] Small changes within the physiological range of gap-junction coupling (eg, directional differences caused by anisotropy, or presence of connective tissue septae) result in significant dispersions that are similar to values reported in the literature.[23,25] In this regard, experiments designed to investigate the effects of gap-junction coupling (through application of uncouplers or coupling enhancers) could provide important information regarding APD heterogeneity in the intact tissue.

The results reported in this study were obtained mainly from a multicellular fiber consisting of equal segments of cell types. We have also conducted studies with a smaller/larger number of M cells. Results indicate that the smaller the M-cell region, the smaller the APD dispersion. However, increasing the M region beyond 30 cells did not enhance APD dispersion any further.

Significance of I_{Ks}:I_{Kr} Heterogeneity to Arrhythmogenesis

APD is an important factor in arrhythmogenesis. Heterogeneity of APD and the resulting dispersion of refractoriness

across the ventricular wall could provide the substrate for unidirectional block and reentrant arrhythmias.[26] In addition, adaptation of APD can influence the degree of head-tail interaction during reentry and the stability of the reentrant circuit.[27] As seen in Figures 2, 3, and 7, changes in the density of I_{Ks} could result in dramatic changes in APD and its rate dependence. For example, cells with decreased I_{Ks} increase APD disproportionately as stimulation rate is decreased. In more general terms, cells with smaller density of I_{Ks} are more responsive to pathologies or interventions (eg, the hereditary or acquired long QT syndrome) that cause APD prolongation. The results obtained from the multicellular fiber suggest that a baseline level of APD differences exists even in the normal myocardium. These differences can increase substantially in the presence of reduced intercellular coupling, even if the cellular repolarization properties remain normal. Conversely, the higher susceptibility of M cells to pathologies and interventions that prolong APD suggests that large dispersion can arise in the normally coupled myocardium. Of course, a combination of enhanced cellular heterogeneity and reduced coupling (eg, class III effects in an infarcted heart) can result in extreme levels of APD dispersion.

In the present study, we focus on intrinsic cellular heterogeneities and their interplay with gap-junction coupling in the context of dispersion of repolarization. In the presence of pathologies or interventions that slow repolarization, sufficient APD prolongation can generate EADs,[8,28] preferentially in the M cells. Consequently, M cells could become a source of triggered activity and focal arrhythmias.[8] The focal mechanism and the enhanced APD heterogeneity introduced by the M cells could act synergistically, with an EAD providing the trigger (a premature stimulus) to a substrate that is predisposed to the development of unidirectional block and reentry caused by large APD dispersion.[23] Although the study addresses the issue of I_{Ks}/I_{Kr} heterogeneity in ventricular myocardium and M cells, it is to be noted that Purkinje cells are also very prone to EAD generation.

Limitations of the Study

Of particular importance to myocardial electrophysiological heterogeneity is the variability in the density of I_{to}, I_{Kr}, and I_{Ks}, which are major players in determining the shape and duration of the AP. This study focuses on heterogeneities in I_{Kr} and I_{Ks} and their effects on APD and its rate dependence. Such heterogeneities have been observed in guinea pig ventricular myocardium, in which I_{to} is absent.[5] The use of a guinea pig–type myocyte model in this study permitted us to investigate the effects of I_{Kr} and I_{Ks} variations without the complicating influences of I_{to}. Clearly, the role of I_{to} in influencing APD and its rate dependence also needs to be investigated, especially in the context of transmural heterogeneity of action potential morphology ("spike and dome" configuration[1]).

It is well established that I_{Ks} decays more slowly than I_{Kr} in the guinea pig but decays more rapidly than I_{Kr} in canine ventricular myocytes. Therefore the conclusions of this study do not necessarily apply to canine myocytes. However, this study shows that rate-dependent shortening of APD results not only from I_{Ks} accumulation but also from a greater outward I_{NaCa} at rapid rates. It is likely that in the absence of I_{Ks} accumulation (eg, in the canine) the main mechanism of rate-dependent APD shortening is a larger outward I_{NaCa} at fast rates.

The role of gap-junction coupling in APD heterogeneity was studied in a 1-dimensional fiber. This is a simplified model that allowed us to investigate this phenomenon at the cellular and ionic channel levels and to establish the principle that APD dispersion is highly sensitive to the degree of intercellular coupling. Moreover, 1-dimensional propagation that can be simulated in a 1-dimensional model occurs frequently in the 3-dimensional heart when broad-plane waves are generated. Importantly, this is the situation during normal sinus rhythm in which planar waves created by the Purkinje network propagate from endocardium to epicardium. A similar situation occurs in the wedge preparation used extensively[25] to study myocardial heterogeneity. It is possible that the higher degree of connectivity in the 3-dimensional myocardium acts to reduce APD dispersion under conditions of tight coupling. However, the principle of strong dependence of APD dispersion on gap junction coupling should carry over to the 3-dimensional myocardium. It should also be emphasized that local dispersion on a cellular scale is involved in the generation of unidirectional block and possibly reentry. Even in the presence of complex 3-dimensional global wave fronts, local excitation can be 1-dimensional in nature. This is particularly true in the presence of structural complexities and pathologies, such as a narrow fiber connecting islands of surviving tissue in an infarct.

Appendix

Formulation of I_{Ks}

$$I_{Ks}=\bar{G}_{Ks}\times xs1\times xs2\times(V-E_{Ks})$$

$$E_{Ks}=(RT/F)\times\ln(([K^+]_o+P_{Na,K}\times[Na^+]_o)/([K^+]_i+P_{Na,K}\times[Na^+]_i));\quad P_{Na,K}=0.01833$$

$$\bar{G}Ks=0.433\times(1+0.6/(1+(3.8\text{E}-5/[\text{Ca}^{2+}]_i)^{1.4}))\quad\text{———Control cell, CT1}$$

$$x_{s\infty}=1/\{1+\exp[-(V-1.5)/16.7]\}$$

$$\tau_{xs1}=1/\{7.19\times10^{-5}\times(V+30)/[1-\exp(-0.148(V+30))]+1.31\times10^{-4}(V+30)/[\exp(0.0687(V+30))-1]\}$$

$$\tau_{xs2}=4\times\tau_{xs1}$$

CICR From Junctional SR (JSR)

Recent experimental evidence[29] has suggested that the apparent "threshold" for calcium release from the SR is due to the degree of recruitment of local SR release channels. It follows that there is always calcium release triggered by calcium entry, and the release becomes significant as calcium entry increases. In light of these findings we have modified the release criterion such that there is always a small release, which increases with the increase in calcium entry. This is achieved by adding a "tail" to the calcium entry–dependent term of the SR calcium release conductance, G_{rel} (see Reference 13). The modified formulation of the SR release current, I_{rel}, is given below.

$$I_{rel}=G_{rel}([\text{Ca}^{2+}]_{JSR}-[\text{Ca}^{2+}]_i)\text{mmol/L/ms}.$$

If $\Delta[Ca^{2+}]_{i,2} > \Delta[Ca^{2+}]_{i,th}$ 2 ms after the time of V_{max},

$$G_{rel} = \bar{G}_{rel} \times \frac{\Delta[Ca^{2+}]_{i,2} - 0.18 \times 10^{-3}}{K_{m,rel} + \Delta[Ca^{2+}]_{i,2} - 0.18 \times 10^{-3}} \times (1 - \exp[-t/\tau_{on}]) \times \exp[-t/\tau_{off}]$$

If $0 < \Delta[Ca^{2+}]_{i,2} < \Delta[Ca^{2+}]_{i,th}$ 2 ms after the time of V_{max},

$$\Delta[Ca^{2+}]_i = \Delta[Ca^{2+}]_{i,2} \times 10^3$$

$$G_{rel} = \bar{G}_{rel} \times (7.5 \times (\Delta[Ca^{2+}]_i)^3 - (\Delta[Ca^{2+}]_i)^2 + 0.1 \times (\Delta[Ca^{2+}]_i)) \times (1 - \exp[-t/\tau_{on}]) \times \exp[-t/\tau_{off}]$$

If $\Delta[Ca^{2+}]_{i,2} \leq 0$ 2 ms after the time of V_{max},

$G_{rel} = 0.0$ $\Delta[Ca^{2+}]_{i,th} = 0.242$ μmol/L; $K_{m,rel} = 0.8$ μmol/L; $\tau_{on} = \tau_{off} = 2$ ms; $\bar{G}_{rel} = 18$ ms^{-1} for voltage clamp simulations; and $\bar{G}_{rel} = 60$ ms^{-1} for action potential simulations.

Acknowledgments

This study was supported by National Institutes of Health grants ROI-49054 and R37-33343 (National Heart, Lung, and Blood Institute) to Y.R.

References

1. Litovsky SH, Antzelevitch C. Rate dependence of action potential duration and refractoriness in canine ventricular endocardium differs from that of epicardium: role of the transient outward current. *J Am Coll Cardiol*. 1989;14:1053–1066.
2. Eddlestone GT, Zygmont AC, Antzelevitch C. Larger late sodium current contributes to the longer action potential of the M-cell in canine ventricular myocardium. *PACE*. 1996;19:569. Abstract.
3. Liu DW, Antzelevitch C. Characteristics of the delayed rectifier current (*IKr* and IKs) in canine ventricular epicardial, midmyocardial, and endocardial myocytes: a weaker IKs contributes to the longer action potential of the M cell. *Circ Res*. 1995;76:351–365.
4. Brahmajothi MV, Morales MJ, Reimer KA, Strauss HC. Regional localization of ERG, the channel protein responsible for the rapid component of the delayed rectifier, K+ current in the ferret heart. *Circ Res*. 1997; 81:128–135.
5. Sicouri S, Quist M, Antzelevitch C. Evidence for the presence of M cells in the guinea pig ventricle. *J Cardiovasc Electrophysiol*. 1996;7:503–511.
6. Sicouri S, Antzelevitch C. A subpopulation of cells with unique electrophysiological properties in the deep subepicardium of the canine ventricle: the M cell. *Circ Res*. 1991;68:1729–1741.
7. Drouin E, Charpentier F, Gauthier C, Laurent K, Le Marec H. Electrophysiologic characteristics of cells spanning the left ventricular wall of human heart: evidence for presence of M cells. *J Am Coll Cardiol*. 1995;26:185–192.
8. Sicouri S, Antzelevitch C. Drug-induced afterdepolarizations and triggered activity occur in a discrete subpopulation of ventricular muscle cells (M cells) in the canine heart: quinidine and digitalis. *J Cardiovasc Electrophysiol*. 1993;4:48–58.
9. Sanguinetti MC, Jurkiewicz NK. Two components of cardiac delayed rectifier K+ current: differential sensitivity to block by class III antiarrhythmic agents. *J Gen Physiol*. 1990;96:195–215.
10. Zeng J, Laurita KR, Rosenbaum DS, Rudy Y. Two components of the delayed rectifier K+ current in ventricular myocytes of the guinea pig type: theoretical formulation and their role in repolarization. *Circ Res*. 1995;77:140–152.
11. Sanguinetti MC, Curran ME, Spector PS, Keating MT. Spectrum of HERG K+ channel dysfunction in an inherited cardiac arrhythmia. *Proc Natl Acad Sci U S A*. 1996;93:2208–2212.
12. Duggal P, Vesely MR, Wattanasirichaigoon D, Villafane J, Kaushik V, Beggs AH. Mutation of the gene for IsK associated with both Jervell and Lange-Nielsen and Romano-Ward forms of long-QT syndrome. *Circulation*. 1998;97:142–146.
13. Luo CH, Rudy Y. A dynamic model of the cardiac ventricular action potential, I: simulations of ionic currents and concentration changes. *Circ Res*. 1994;74:1071–1096.
14. Luo CH, Rudy Y. A dynamic model of the cardiac ventricular action potential, II: afterdepolarizations, triggered activity, and potentiation. *Circ Res*. 1994;74:1097–1113.
15. Tohse N. Calcium-sensitive delayed rectifier potassium current in guinea pig ventricular cells. *Am J Physiol*. 1990;258:H1200–H1207.
16. Nitta J, Furukawa T, Marumo F, Sawanobori T, Hiraoka M. Subcellular mechanism for Ca^{2+}-dependent enhancement of delayed rectifier K+ current in isolated membrane patches of guinea pig ventricular myocytes. *Circ Res*. 1994;74:96–104.
17. Shaw RM, Rudy Y. Ionic mechanisms of propagation in cardiac tissue: roles of the sodium and L-type calcium currents during reduced excitability and decreased gap junction coupling. *Circ Res*. 1997;81:727–741.
18. Kieval RS, Spear JF, Moore EN. Gap junctional conductance in ventricular myocyte pairs isolated from postischemic rabbit myocardium. *Circ Res*. 1992;71:127–136.
19. Jurkiewicz NK, Sanguinetti MC. Rate-dependent prolongation of cardiac action potentials by a methanesulfonanilide class III antiarrhythmic agent: specific block of rapidly activating delayed rectifier K+ current by dofetilide. *Circ Res*. 1993;72:75–83.
20. Cohen CJ, Fozzard HA, Sheu SS. Increase in intracellular sodium ion activity during stimulation in mammalian cardiac muscle. *Circ Res*. 1982;50:651–662.
21. Harrison SM, Boyett MR. The role of Na+- Ca+ exchanger in the rate dependent increase in contraction in guinea-pig ventricular myocytes. *J Physiol*. 1995;482:555–566.
22. Anyukhovsky EP, Sosunov EA, Rosen MR. Regional differences in electrophysiologic properties of epicardium, midmyocardium and endocardium: in vitro and in vivo correlations. *Circulation*. 1996;94: 1981–1988.
23. El-Sherif N, Caref EB, Yin H, Restivo M. The electrophysiological mechanism of ventricular arrhythmias in the long QT syndrome: tridimensional mapping of activation and recovery patterns. *Circ Res*. 1996; 79:474–492.
24. Salama G, Kanai AJ, Huang D, Efimov IR, Girouard SD, Rosenbaum DS. Hypoxia and hypothermia enhance spatial heterogeneities of repolarization in guinea pig hearts: analysis of spatial autocorrelation of optically recorded action potential durations. *J Cardiovasc Electrophysiol*. 1998; 9:164–183.
25. Shimizu W, Antzelevitch C. Sodium channel block with mexiletine is effective in reducing dispersion of repolarization and preventing torsade de pointes in LQT2 and LQT3 models of the long QT syndrome. *Circulation*. 1997;96:2038–2047.
26. Surawicz B. Electrophysiologic substrate of torsade de pointes: dispersion of repolarization or early afterdepolarizations. *J Am Coll Cardiol*. 1989; 14:172–184.
27. Rudy Y. Reentry: insights from theoretical simulations in a fixed pathway. *J Cardiovasc Electrophysiol*. 1995;6:294–312.
28. January CT, Riddle JM. Early afterdepolarizations: mechanism of induction and block: a role for L-type Ca2+ current. *Circ Res*. 1989;64: 977–990.
29. Cannell MB, Cheng H, Lederer WJ. The control of calcium release in the heart muscle. *Science*. 1995;268:1045–1049.

Effects of I_{Kr} and I_{Ks} Heterogeneity on Action Potential Duration and Its Rate Dependence : A Simulation Study

Prakash C. Viswanathan, Robin M. Shaw and Yoram Rudy

Circulation. 1999;99:2466-2474
doi: 10.1161/01.CIR.99.18.2466
Circulation is published by the American Heart Association, 7272 Greenville Avenue, Dallas, TX 75231

Print ISSN: 0009-7322. Online ISSN: 1524-4539